Synthesis and characterization of Bi_2O_3 NPS and photocatalytic application with methylene blue

F. S. Ali[a,*], M. Ragamathunnisa[d], F. Al Marzouqi[c], A. R. M. Jahangir[d], A. Ayeshamariam[e,*], K. Kaviyarasu[f,g]

[a]*Department of Chemistry, Khadir Mohideen College, Adirampattinam. 614701(Affiliated to Bharathidasan University, Tiruchirappalli) India*

[b]*Department of Physics, Government Arts College for Women (Auto), Pudukkottai, 622001, India*

[c]*Department of Chemistry, College of Science, Sultan Qaboos University, Muscat, Oman*

[d]*Biyaq Oilfield Services LLC Post Box: 795, Mina Al Fahal PC, 116, Muscat, Sultanate of Oman*

[e]*Department of Physics, Khadir Mohideen College, Adirampattinam. 614701(Affiliated to Bharathidasan University, Tiruchirappalli) India*

[e]*Kasinathan Kaviyarasu, UNESCO-UNISA Africa Chair in Nanosciences/Nanotechnology Laboratories, College of Graduate Studies, University of South Africa (UNISA), Muckleneuk Ridge, P O Box 392, Pretoria, South Africa*

[f]*Nanosciences African network (NANOAFNET), Materials Research Group (MRG), iThemba LABS-National Research Foundation (NRF), 1 Old Faure Road, 7129, P O Box 722, Somerset West, Western Cape Province, South Africa*

Bismuth oxide nanoparticle was synthesized by Hydrothermal method, with two different molar ratio of precipitating agent of NaOH which decided the variations of two samples (1:5) and (1:6) was added to observe its effect on structural, optical and photocatalytic behaviour. So the prepared bismuth oxide nano particle was characterized by X-ray Diffractometer to study about its crystalline properties. The crystal size was observed as 30.7 and 42.84 nm, The optical properties were characterized by using UV-Vis spectrometer and its band gap value was calculated as 2.74 eV and 2.42 eV respectively. Morphological studies were obtained by using scanning electron microscopy and the elemental X-ray analysis confirmed the proportions of Bi_2O_3 nanoparticles of two samples (1:5) and (1:6). FTIR Spectrometer studies explained the condensation of OH group accompanied by the formation of Bi_2O_3 which is strongly dependent on the pH of reaction. A lattice change was observed, symmetric and asymmetric bonds were analysed by using FTIR spectrometer. The binding energy and its energy level were analysed by using X-ray Photo electron Spectroscopy and its value was 292 and 534 eV, and also the hydrothermal synthesised Bi_2O_3 NPs was used to analysed the photocatalytic degradation of Methylene blue under the irradiation of LED white light.

(Received March 12, 2021; Accepted July 23, 2021)

Keywords: Photcatalystic studies, Bi_2O_3 NPs, SEM and EDAX

1. Introduction

The controlled synthesis of Bi_2O_3 nanoparticles in mono disperse range is still a challenge**.** Chemical synthesis is a straight forward synthesis route and the temperature is the main parameter which easily hydrolyses to starting solution for the well defined nanoscaled Bi_2O_3. The synthesis of Bi_2O_3 NPs with high yield approach shows the promising activity to the photocatalytic degradation of dyes in aqueous solution. The influence of crystallite size prepared by the

* Corresponding authors: fowziyaonline@yahoo.co.in; ayeshamariamkmc@gmail.com

hydrothermal synthesis of the catalyst with dye concentration of MB was investigated by using organic pollutants of phenol, 4-chloro phenol and 4- nitro phenol in water [1].

Recently many studies reported that Bi_2O_3 nano materials possessed many applications in specific detection of diseases, and tailored nanostructures of Bi_2O_3 for electronic, medical, biological sensors and other pertinent applications. It provides information about the trapped charged recombination sites related to metastable defects in the lattice depending on whether the entrapping process is due to heat. The existence of the oxygen vacancy in Bi_2O_3 also influences the catalytic activity. Thus small variation in the lattice structure due to the presence of inclusion impurities, substituted ions, surface defects in *ppm* concentration reveals successful degradation of photocatalytic properties. A number of studies Bi_2O_3 have been conducted on reaction optimization and structural modification (e.g., metal doping or material hybridization) to improve the photoactivity and energy conservation.

Hai Bang Truong et al., reported that the complex degradation behavior of natural organic matter (NOM) was explored using photocatalytic oxidation systems with a novel catalyst based on a hybrid composite of zinc-bismuth oxides and g-C_3N_4 (ZBO-CN). The photooxidation system demonstrated the effective removal of NOM under low-intensity visible light irradiation, presenting removal rates of 53-74% and 65-88% on the basis of dissolved organic carbon (DOC) and the UV absorption coefficient (UV254), respectively, at 1.5 g/L of the catalyst [2].

A novel $Cu_2O/TiO_2/Bi_2O_3$ ternary nanocomposite was prepared, in which copper oxide improves the visible light absorption of TiO_2 and bismuth oxide improves electron–hole separation. The ternary composite exhibited extended absorption in the visible region, as determined by UV–Vis diffuse reflectance spectroscopy. Improved charge carrier separation and transport were observed in the $Cu_2O/TiO_2/Bi_2O_3$ ternary composite using electrochemical impedance spectroscopy and photocurrent analysis. The synergistic effect of improved visible absorption and minimal recombination was responsible for the enhanced performance of the as-synthesized ternary nanocomposites [3].

The BiOI-rGO photocatalyst exhibited high crystallinity with tetragonal phase of BiOI. A significant quenching in the photoluminescence intensity of rGO supported BiOI photocatalyst confirmed the effective suppression of electron-hole pair recombination. The optimized rGO (4 wt%) loaded BiOI photocatalyst significantly improved the photocatalytic activity (>85%) towards the degradation of methyl orange (MO) dye compared to that of pristine BiOI (>29%). Thus, around three folds enhancement in the photocatalytic activity of BiOI–rGO (4 wt%) catalyst was mainly attributed to ultrafast separation of electron–hole pairs and rapid transportation of carriers by rGO support [4].

All the information about the characterization of structural and phase information were predominated to study optical properties of the prepared nano particles by using X-ray diffractometer. The multipilicity of bonds due to emission and excitation spectra were characterized by using Raman spectrometer. These studies constitute the basis of developing applications of photocatalytic properties. The aim of the work describes to investigate the impact of Bi_2O_3 NPs samples (1:5) and (1:6) which determines whether the mechanism of Bi_2O_3 interaction in degradation process is similar or dissimilar with dissolution of Bi^{3+} ions into the dye solution and compared with the reported earlier results [5].

The FTIR analysis of effective scientific technique which explain the functional group with a strong dipole asymmetric stretching vibration and analysis whether it was good agreement with early reported results. We reported here hypothesis of photocatalytic degradation, increasing the concentration of reactant ions, rate of nucleation growth. The influence of crystallite size prepared by the hydrothermal synthesis of the catalyst with dye concentration, Methylene Blue (MB) was investigated by using organic pollutants of phenol, 4- chloro phenol and 4- nitro phenol in water. Wide variety of synthesis techniques have already been developed to produce Bi_2O_3 in powder and thin film form, its various properties strongly depends on its structure including the crystal size, orientation, morphology and density. Among all the synthetic routes, hydrothermal synthesis should be further improved, to meets the requirement of environmental production [6].

MB is a water soluble dye which widely used in pharmaceuticals, food industries and textile printing. The safe removal of MB dye is the prime aim of our present study. This study concentrate to examine the effect of pH value and the reaction of photocatalytic performance by

using Bi_2O_3 NPs was reported here. They removal of dye to decompose by the photocatalytic process explains the separation of photogenerated charge carriers for enhancing the photocatalytic activity. However micron grain sized Bi_2O_3 which act as a semiconductor so its surface area is very low and photogenerated charge carriers cannot be transferred for the fast charge carrier's recombination. Phase composition influencing the crystal structure and crystal growth giving much specified morphology, favorable linked polar phases acting as capping agents. In this work we present a facile hydrothermal approach with improved needle shape morphology having diameter of 500 nm incorporated with coordinating reagent for the formation of proposed experimental results [7].

2. Experimental methods

2.1. Synthesis of Bi_2O_3Nano particles

Nano particles were synthesized using analytical grade Bismuth (III) nitrate ($Bi(NO_3)_3.6H_2O$,Sigma Aldrich,99%), sodium hydroxide(NaOH, Sigma Aldrich,99%) and Nitric acid (Sigma Aldrich,68%) without further purification and Ultra-pure water. In a hydrothermal synthesis, 1 mmol of $Bi(NO_3)_3.6H_2O$ was dissolved in 50 mL of 0.3M Nitric acid, then the solution was sonicated about 15 minutes, at room temperature with purpose to achieve homogeneous solution. Then, 0.2 M of sodium hydroxide solution of 5-6 mmol (1:5 to 1:6 molar ratio of Bi $(NO_3)_3.5H_2O$ to NaOH) was added drop by drop into the clear solution under vigorous stirring. During the reaction, the pH of the mixture increases gradually and attained approximately above 10, precipitation process started to form white precipitate. After 30 min continuous stirring, white precipitate obtained was transferred into autoclave with Teflon lining and kept at 160º C for 12 hours for hydrothermal treatment. The autoclave was cooled to room temperature naturally. The yellow precipitate was obtained by centrifugation (6 min with 7500 rpm) and washed several times with ultra-pure water and dried at 80º C for 12 hours. Finally, the products were calcined at 350º C for 3 hours for further characterization [8].

2.2. Characterization

The crystalline properties of the synthesized Bi_2O_3 nano particles were studied by XRD using a Bruker (D5005) X-ray diffractometer equipped with graphite monochromatized CuKα radiation (λ =1.54056Å). An accelerating voltage of 40 kV and emission current of 30 mA were adopted for the measurements. In addition to XRD, FTIR spectroscopy measurements were also performed to confirm the structure of the Nano particles. The morphology of the crystal was characterized by SEM. The SEM measurements were performed by a Hitachi S-4800 high resolution (HR) field emission scanning electron microscope. The FE–SEM equipment was also furnished with an EDAX spectrometer that was used for elemental analysis. Absorption spectra of the samples in the diffused reflectance spectrum (DRS) mode were recorded in the wavelength range of 200- 1000 nm using a spectrophotometer (Jasco V 670), with $BaSO_4$ as a reference. From the adsorption edge, the band gap values were calculated by extrapolation.

2.3. Photocatalytic activity

Photocatalytic activity of pure Bi_2O_3 nano particle were examined by the rate of degradation of MB under the effect LED white light irradiation. All photo catalytic reaction were performed out in photo catalytic reactor system, which consists of a cylindrical borosilicate glass reactor vessel with volume of 250 *mL*, a cooling water jacket, and a LED white light, Institute of Electric Light Source, Beijing)positioned axially at the centre as a visible light. The reaction temperature was kept at 25° C by circulating the cooling water. A special glass frit as an air diffuser was fixed at the reactor to uniformly disperse air into the solution. For each run the reaction suspension was freshly prepared by adding 0.250 g of catalyst into 250 mL of initial concentration of 5 mg/L of Methylene Blue. After the degradation reaction, filtration was done for all samples using syringe and syringe filter 0.45 µm to remove any precipitated particles. The filtrate was analysed by an UV-Vis spectrometer (UC-2450-SHIMADZU). The maximum characteristic absorption wavelength of MB was positioned [9].

3. Result and discussion

3.1. XRD

Hydrothermally synthesised Bismuth oxide nanocrystals were examined by using powder x-ray diffraction spectrometry. XRD patterns of the as synthesised samples shown in Figure.1.The X-ray diffraction pattern of Bi_2O_3 materials exhibited reflection peaks at 31.923 of glancing angle. All reflection peaks can be well indexed with a pure tetragonal phase of crystalline Bi_2O_3, which are in good agreement with the fiber structure of tetragonal phase (JCPDS card No: 65-4028). The broad reflection peaks suggested that the materials are nano crystalline structure. The crystalline of Bi_2O_3 NPs is nearly 42 nm, which shows that the product consists of needle shaped nano crystals. The additional reflection peaks indicates that when OH ions are used for the preparation of nano crystalline structure with additional phase of Bi_2O_3 is strongly influenced by the variation of pH solution caused by particular molar ratio of NO_3^- and hydroxyl ions. In our case the high concentration of reducing agent NaOH which is used to raise the pH value of given solution between 8 to 10 to reach the optimum condition [10]. The temperature of the hydrothermal synthesis increasing concentration of aqueous solution and Bi^{3+} ions species into pure obtained phase suggesting that this 160º C optimum temperature of the solvent are used for stabilizing the agent. The materials exhibited crystalline structure of Tetragonal with the lattice constants 3.850 Aº and 12.250 Aº which is good agreement with JCPDS No 65-4028. Calculated structural parameters were tabulated in Table 1.

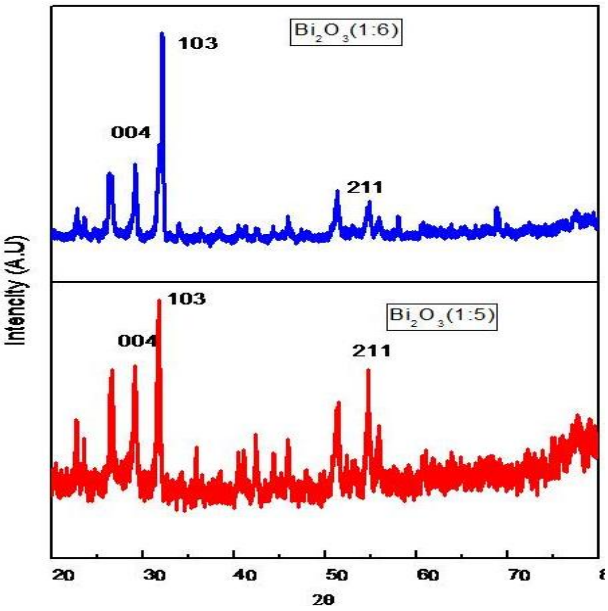

Fig. 1. XRD Analysis of Bi_2O_3 Nanoparticle.

Table 1. XRD Analysis of Bi_2O_3 Nanoparticle.

Samples	2θ		d-spacing		Crystal size (nm)	lattice constant		hkl
	Obs	Std JCPDS	d_{obs}	d_{std} JCPDS		a Aº	c Aº	
Bi_2O_3(1:5)	32.10	31.923	2.811	2.8012	30.70	3.8518	12.922	103
Bi_2O_3(1:6)	31.768	31.923	2.784	2.8012	42.84	3.8489	12.107	103

3.2. XPS

The XPS spectra of Bi_2O_3 NPs were obtained and shown in Fig. 2. There are two asymmetrical peaks observed at 292 eV and 198 eV correspond to Bi 4f orbitals band its electro chemical reduction of new peaks were consistent with Bi 4f spectra for the Bi metal. This peak at 534 eV correspond to Bi ions and its signal voltage is assigned to Bi^{3+} ion which are in good agreement with reported XPS analysis of Bi_2O_3 NPs. The surface analysis of Bi_2O_3 NPs and its peaks were resulted there is no shoulder of Bi $4f_{7/2}$ peaks related to either bivalent or tetravalent states, instead it gives Bi $4f_{5/2}$ of Bi_2O_3 gives a report as the surface of the prepared particle were consist of pure Bi_2O_3 and they were not any BiO and Bi_2O_5 phases [11].

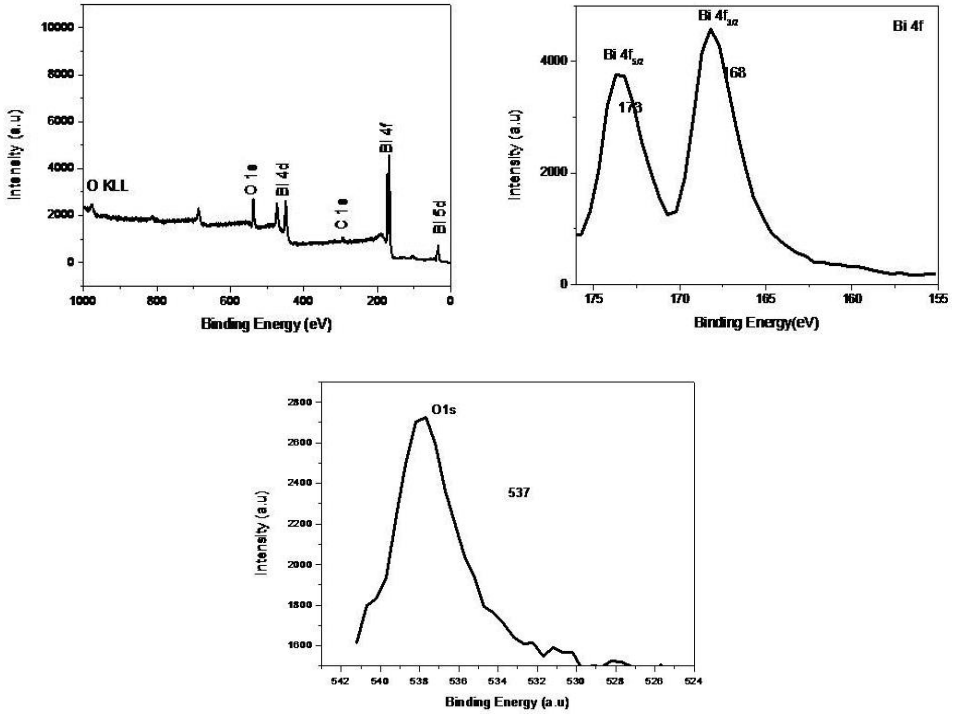

Fig. 2. XPS Analysis of Bi_2O_3 (1:6).

The valence band offset ΔEv can be described by the formula,

$$\Delta E_v = (4f - V_{BM}) + \Delta E_{CL}$$

CL= core level

ΔE_{CL} = Energy difference between Bi 4f (Bi_2O_3) core levels which are measured on this sample by XPS spectra. V_{BM} position in the Valence band spectra was determined from the analysis and its values are 2.74 eV to 2.42 eV respectively which is well matched with the results of bandgap of Bi_2O_3. The linear extrapolation of the leading edges of valence band spectra were determined according to linear extrapolation so the leading edges of the valence band spectra recorded to the base lines [12].

3.3. SEM

The morphological studies of Bi_2O_3 samples are shown in Fig. 3(a-b). From the SEM image only isolated sub- micron spherical structure with average diameter of 2 μm are observed. The appearance of spherical distribution could be attributed to the formation of co ordination compounds of bismuth and oxygen ions.

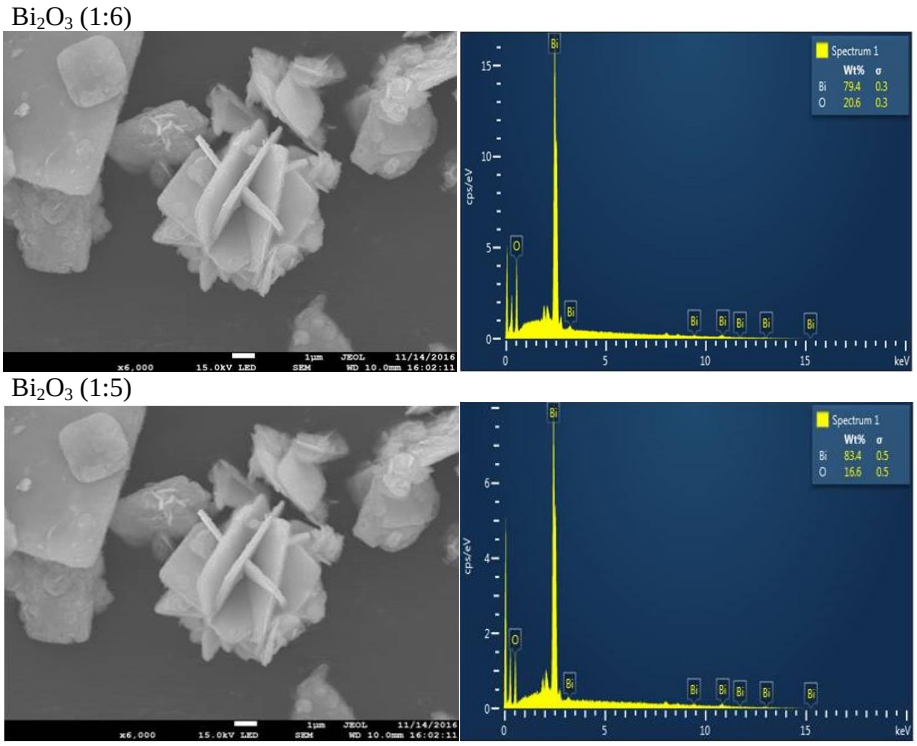

Fig. 3. SEM analysis of Bi_2O_3 Nanoparticles for the proportion ratio (1-6) and (1-5).

Table 2. EDAX Analysis of Bi_2O_3 Nanoparticle.

Element Bi_2O_3(1:6)	Weight %	Element Bi_2O_3(1:5)	Weight %
Bi	79.4	Bi	83.4
O	20.6	O	16.6
TOTAL	100	TOTAL	100

The rate of change of nucleation and crystal formation was rationally concluded that the surfactant and oxidizing agent an important key factor for the formation of fibre like structure [13]. A perfect geometrical shape and well defined boundary of the structure are the important parameters that could be measured with the different variation of concentration of Bi_2O_3 .So that the morphology obtained are treated with different variation of concentration of source materials.

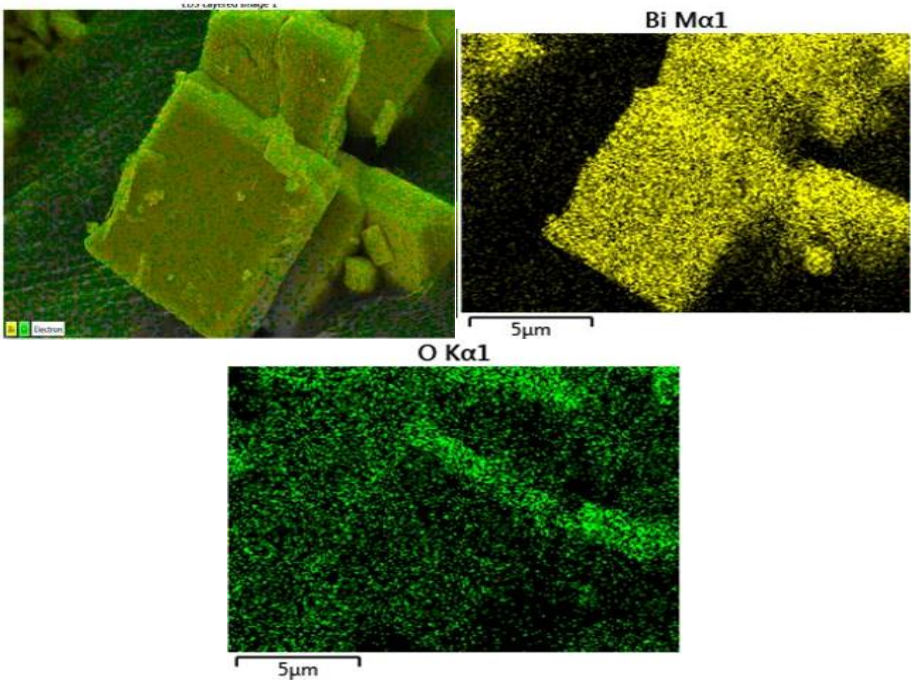

Fig. 4. SEM Mapping of Bi_2O_3 NPs proportion ratio of (1-5) and (1-6).

3.4. UV DRS

The UV-Visble studies of three different concentrations of the samples were carried out for the calculation of bandgap values by using Tauc plots. The absorption edge for the three samples is different and was nearly 2.74 and 2.42 eV. This variation is influenced by the variation of crystallite size. The direct bandgap was carried out for the allowed transition to study the absorption coefficient, percentage of transition and the bandgap value. The typical plot the absorption coefficient Vs wavelength, $(\alpha h\nu)^2$ Vs $h\nu$ and percentage of transmittance Vs wavelength represents the allowed transition of Bi_2O_3 for the three different variation with proposed semiconductor behavior of our nano fibres [14].

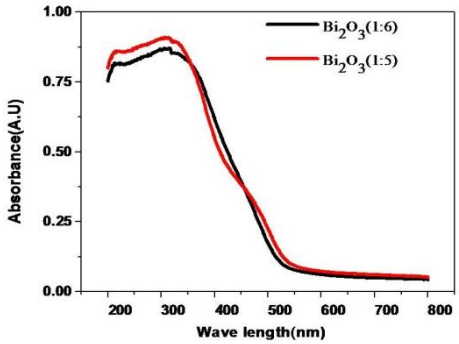

Fig. 5. a Absorbance curve of Bi_2O_3 (1-5 and 1-6).

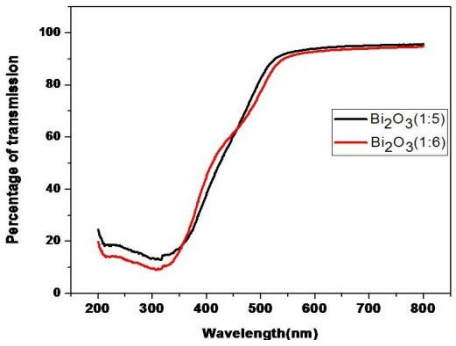

Fig. 5. b Transmittance curve of Bi_2O_3 (1-5 and 1-6).

At the same time the Fermi level of three samples is related to the oxygen pressure due to using DRS reflectance spectra. For an integrating sphere exclude the diffuse scattering effects. The intending band alignment would always be a dominant behaviour to study the band alignment between bismuth and oxygen ions. It is worthwhile to known that the surface area is nearly $25m^2/g$ for the two samples which results in decreasing crystallite size of phase transformation, this phase for these two samples show a thermodynamically spontaneous transformation for the design and optimum surface area of the samples are 2.74 and 2.42 eV [15].

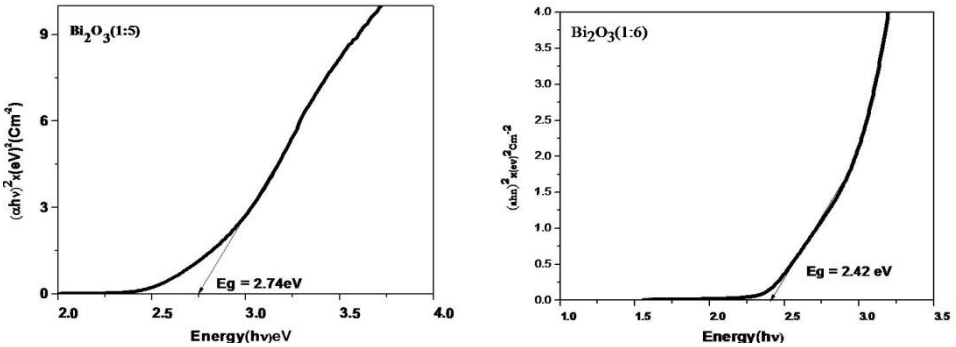

Fig. 5. c UV-Vis Analysis and its band gap of Bi_2O_3 (1-5 bandgap 2.74 eV and 1-6 bandgap 2.42 eV).

3.5. FTIR

The phase composition and the vibrational frequency were formed by using FTIR spectroscopy $Bi(NO_3)_3$ which can be transformed into single phase Bi_2O_3 and its OH group was released by the oxidation reactions of reagent dissolved in the preparation. The distilled water OH group was observed for the influence of composition of reaction products containing large amounts of hydroxyl group with high specific surface area 25 m^2g^{-1} were treated at the pH condition of 6. Suppose the pH is greater than 7 the IR region showed no OH group in the products the morphology of the product of fiber like structure inferred, the particles were prepared under acidic condition [16].

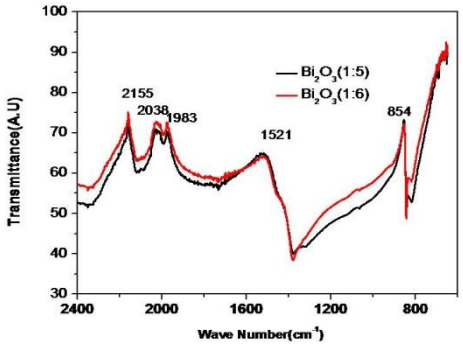

Fig. 6. FTIR Analysis and its band gap of Bi_2O_3 (1-5 and 1-6).

The crystalline product containing bismuth and oxygen ions having fibre shaped particles resulted a possible reaction mechanism by hydration and were followed by hydrolysis. The condensation of OH group accompanied by the formation of Bi_2O_3 is strongly dependent on the pH of reaction medium. The accelerated Bi^{3+} ion causes non conventional volume of reaction by the applied temperature inside the chamber [17].

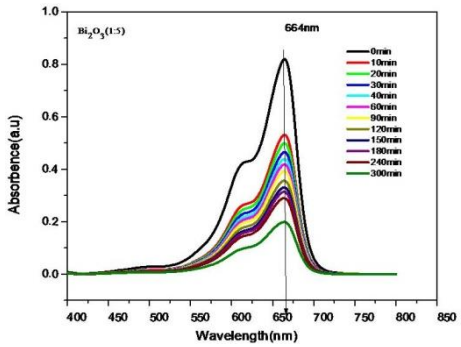

Fig. 7. Absorbance curve of Bi_2O_3 (1-5).

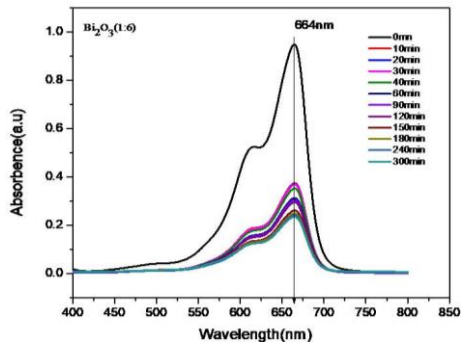

Fig. 8. Absorbance curve of Bi_2O_3 (1-6).

The photocatalytic activity of the as-prepared Bi_2O_3 nanoparticles of different molar ratio was examined by the degradation of methylene blue (MB) under visible light irradiation (Figs. 7-8). It is found that only about 10% MB was degraded after 30 minutes degradation with photocatalyst in the absence of visible light irradiation (Figs. 7-8). As Bi_2O_3 nanoparticle of 1:5 molar ratio with a bandgap of Bi_2O_3 (1-5 bandgap 2.74 eV and 1-6 bandgap 2.42 eV) cannot be excited in the absence of visible light irradiation, the photodegradation of MB over 1:5 molar ratio of Bi_2O_3 in the absence of visible light irradiation shows negligible efficiency. Noticeably, 1:6

ratio also display low efficiency for MB degradation due to its low valence band location, although it has been considered an excellent visible-light-driven photocatalyst [18].

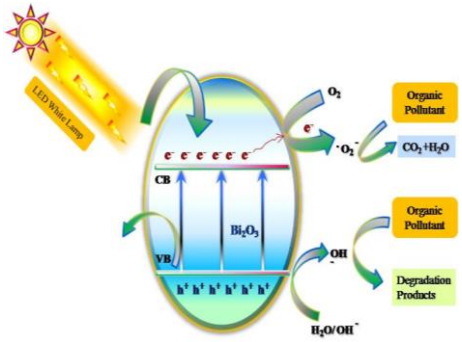

Fig. 9. Schematic diagram of Photocatalytic effect of Bi_2O_3 NPs.

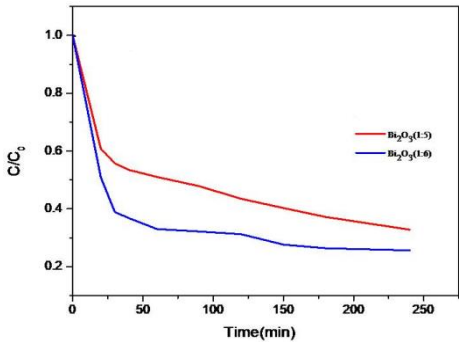

Fig. 10. Variation of graph with Time (min) for the degradation ratio of C/C_0.

In a typical activity test a defined amount of photocatalyst was suspended in 100 mL of MB solution [19]. The suspension was left in dark condition for 2 hours to reach the adsorption equilibrium, and then photocatalytic reaction was initiated under visible light up to 250 min. The experiments were performed with a pyrex cylindrical photoreactor (ID = 2.8 cm) equipped with an air distributor device (Q_{air}=150 cm^3/min (STP)), a magnetic stirrer to maintain the photocatalyst suspended in the aqueous solution, and a temperature controller. The photoreactor was irradiated by a strip composed by 30 white light LEDs (nominal power: 6 W) with wavelength emission in the range 400–800 nm or by a similar number of blue light LEDs (nominal power: 6 W) with wavelength emission in the range 400–550 nm. The LEDs strip was positioned around the reactor so that the light source uniformly illuminated the reaction volume. The schematic diagram of Bi_2O_3 NPs is shown in Figure 9 represents degradation principle of it, while the fraction of curve colored in blue evidence the spectrum emission of blue LEDs. On the left side of the same figure a schematic picture of the photocatalytic reactor is presented. Slurry samples were collected at fixed time intervals, and centrifuged for 20 minutes at 4000 rpm for removing photocatalyst particles. The centrifuged samples were analysed to determine the change of dyes concentration, measured with a Perkin Elmer UV-Vis spectrophotometer at 663 nm [20].

As photodegradation of organic pollutant over Bi_2O_3 nanoparticles was dominated as the hole oxidation process, the photogenerated holes over Bi_2O_3 did not exhibit enough over potential for the oxidation of MB, thus leading to the low photocatalytic efficiency. Importantly, it is found that the entire three ratio of the samples exhibit remarkably enhanced photocatalytic activities for MB degradation as compared to these as prepared samples. Among them, Bi_2O_3 nanoparticles with 1:5 molar ratio shows the highest photocatalytic activity and could approximately 80% degrade MB within 3 h. It is believed that Bi_2O_3 (1:5) ratio lattice varies the location of the valence band

somehow; therefore, the photogenerated holes possess higher oxidation power for MB degradation [21].

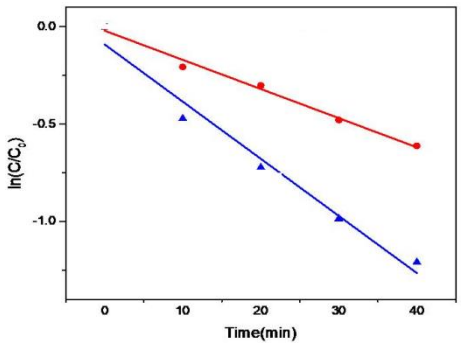

Fig. 11. Degradation of MB dye for Bi_2O_3 NPs of (1:5) and (1:6).

In dark conditions a decrease of MB concentration was observed during the first hour of the test and it was unchanged in the second hour, indicating that the adsorption equilibrium of dye on catalyst surface was reached. The curves show that Bi_2O_3 catalysts have different amounts of MB adsorbed in dark [22]. To explain this last result, the specific area was estimated for the sample (1-5) it was 25 m^2/g, while for (1-6) it was 23 m^2/g. As expected, the amount of organic dye adsorbed increases the higher is the specific surface area, fairly accordingly to the differences in the area values, as shown in Fig. 11.

After the dark period, the solution was irradiated with visible light and the reaction started to occur. Figure 11 shows that Bi_2O_3 NP is slightly effective for MB decolourization, the / reduction being about 10 %, a value similar to that of photolysis reaction (14 %). On the contrary, different proportions of Bi_2O_3 NP photocatalysts exhibited higher photocatalytic activity under visible light irradiation. The order of decolorization activity of Bi_2O_3 NPs after 250 min was as following: (1-5) > (1-6). The final value of MB conversion depends on dye concentration after the dark period.

The decolourization of MB does not necessary correspond to the oxidation and mineralization of the molecule; in fact the reduced form of MB which is colourless can be produced in the presence of light [23]. The lack of coincidence among the best performing samples with respect to either decolorization or mineralization can be the result of different routes followed by MB during irradiation.

4. Conclusion

The nanoparticles Bi_2O_3 was successfully synthesised by the efficient hydrothermal method. The well spherical and also fiber shaped Bi_2O_3 nanoparticles with 30 nm to 42 nm for nanoparticles of different molar ratio were synthesised by this method. It is very simple, time as well as energy saving technique. The XRD pattern shows that the as prepared sample exists in tetragonal lattice. There is no impurities in the prepared sample which is confirmed by Xray photoelectron spectroscopy. Scanning electron micrographs indicates that grains are uniformly distributed. The band gap energy values as prepared bismuth oxide nanoparticles were calculated as 2.74eV and 2.42eV respectively. The photocatalytic degradation activity showed that the synthesised bismuth oxide nanoparticles have a good efficiency to photodegrading MB under LED visible light irradiation.

References

[1] M. M. Patil, V. V. Deshpande, S. R. Dhage, V. Ravi, Materials letters **59**(19-20), 2523 (2005).
[2] H. B. Truong, B. T. Huy, Q. V. Ly, Y. I. Lee, J. Hur, Chemosphere **224**, 597 (2019).
[3] A. K. R. Police, S. P. Vattikuti, K. K. Mandari, M. Chennaiahgari, P. Sharma, D. K. Valluri, C. Byon, Ceramics International **44**(10), 11783 (2018).
[4] R. Vinoth, S. G. Babu, R. Ramachandran, B. Neppolian, Applied Surface Science **418**, 163 (2017).
[5] R. Hernandez-Delgadillo, D. Velasco-Arias, J. J. Martinez-Sanmiguel, D. Diaz, I. Zumeta-Dube, K. Arevalo-Niño, C. Cabral-Romero, International journal of nanomedicine **8**, 1645 (2013).
[6] S. Y. Chai, Y. J. Kim, M. H. Jung, A. K. Chakraborty, D. Jung, W. I. Lee, Journal of Catalysis **262**(1), 144 (2009).
[7] C. D. Ling, Journal of Solid State Chemistry **148**(2), 380 (1999).
[8] R. K. Jha, R. Pasricha, V. Ravi, Ceramics international **31**(3), 495 (2005).
[9] M. Mallahi, A. Shokuhfar, M. R. Vaezi, A. Esmaeilirad, V. Mazinani, AJER **3**(4), 162 (2014).
[10] J. Krishna Reddy, B. Srinivas, V. Durga Kumari, M. Subrahmanyam, Chem Cat Chem **1**(4), 492 (2009).
[11] S. Y. Chai, Y. J. Kim, M. H. Jung, A. K. Chakraborty, D. Jung, W. I. Lee, Journal of Catalysis **262**(1), 144 (2009).
[12] M. Drache, P. Roussel, J. P. Wignacourt, Chemical reviews **107**(1), 80 (2007).
[13] D. Saritha, Y. Markandeya, M. Salagram, M. Vithal, A. K. Singh, G. Bhikshamaiah, Journal of Non-Crystalline Solids **354**(52-54), 5573 (2008).
[14] D. Saritha, Y. Markandeya, M. Salagram, M. Vithal, A. K. Singh, G. Bhikshamaiah, Journal of Non-Crystalline Solids **354**(52-54), 5573 (2008).
[15] C. Pan, X. Li, F. Wang, L. Wang, Ceramics international **34**(2), 439 (2008).
[16] D. Barreca, F. Morazzoni, G. A. Rizzi, R. Scotti, E. Tondello, Physical Chemistry Chemical Physics **3**(9), 1743 (2001).
[17] G. H. Hwang, W. K. Han, S. J. Kim, S.J. Hong, J. S. Park, H. J. Park, S. G. Kang, Journal of Ceramic Processing Research **10**(2), 190 (2009).
[18] Y. Bessekhouad, D. Robert, J. V. Weber, Catalysis Today **101**(3-4), 315 (2005).
[19] R. Li, W. Chen, H. Kobayashi, C. Ma, Green Chemistry **12**(2), 212 (2010).
[20] A. I. El-Batal, G. S. El-Sayyad, A. El-Ghamry, K. M. Agaypi, M. A. Elsayed, M. Gobara, Journal of Photochemistry and Photobiology B: Biology **173**, 120 (2017).
[21] X. Li, Y. Sun, T. Xiong, G. Jiang, Y. Zhang, Z. Wu, F. Dong, F., Journal of catalysis **352**, 102 (2017).
[22] M. Xiong, L. Chen, Q. Yuan, J. He, S. L. Luo, C. T. Au, S. F. Yin, Carbon **86**, 217 (2015).
[23] G. Lin, D. Tan, F. Luo, D. Chen, QA. Zhao, J. Qiu, Z. Xu, Journal of Alloys and Compounds **507**(2), L43 (2010).